Available online at www.sciencedirect.com
SCIENCE DIRECT®
Chaos, Solitons and Fractals 24 (2005) 125–136
CHAOS SOLITONS & FRACTALS
www.elsevier.com/locate/chaos

Bifurcations and chaos of a two-degree-of-freedom dissipative gyroscope

Hsien-Keng Chen [a,*], Zheng-Ming Ge [b]

[a] *Department of Industrial Management, Hsiuping Institute of Technology, 11 Gungye Road, Dali City, Taichung, Taiwan, Republic of China*
[b] *Department of Mechanical Engineering, National Chiao Tung University Hsinchu, Taiwan, Republic of China*

Accepted 6 July 2004

Abstract

The dynamic behaviors of a dissipative gyroscope mounted on a vibrating base are investigated qualitatively and numerically. It is shown that the nonlinear system can exhibit regular and chaotic motions. The qualitative behaviors of the system are studied by the center manifold theorem and the normal form theorem. The co-dimension one bifurcation analysis for the Hopf bifurcation is carried out. The pitchfork, Hopf, and saddle connection bifurcations for co-dimension two bifurcation are also found in this study. Regular and chaotic motions are shown to be possible in the parameter space. Numerical methods are used to obtain the time histories, the Poincaré maps, the Liapunov exponents, and the Liapunov dimensions. The effect of the spin speed of the gyroscope on its dynamic behavior is also studied by numerical simulation in conjunction with the Liapunov exponents, and it has been found that the higher spin speed of the gyroscope can quench the chaotic motion.

1. Introduction

The motion of the gyro is an interesting problem in classical mechanics. Research in the area of gyro dynamics dates back about 100 years, whereas the pioneering paper on the concept of chaotic motion in gyros was already presented in 1981 by Leipnik and Newton [1], showing the existence of two strange attractors. Recently much interest has been focussed on these types of problems. The chaotic motions of a rate gyro and a symmetric heavy gyroscope with harmonic excitation have been found by Ge et al. [2–5]. In 2001, the motion of a symmetric gyro which is subjected to a harmonic vertical base excitation has been studied by Tong et al. [6], with particular emphasis on its nonlinear dynamic behavior without taking into account the damping effect. Very recently, on studying anti-control of chaos in rigid body motion, Chen and Lee [7] introduced a new chaotic attractor. Their studies have proved that chaotic motion can be found in rigid gyro. This paper presents a variety of interesting dynamic phenomena of a dissipative gyroscope excited by a harmonic force with emphasis on its chaotic motion.

* Corresponding author.
E-mail address: kanechen@giga.net.tw (H.-K. Chen).

0960-0779/$ - see front matter © 2004 Elsevier Ltd. All rights reserved.
doi:10.1016/j.chaos.2004.07.028

The concept of chaos has been first introduced by Poincaré [8] to describe orbits in space mechanics. The chaotic behaviors of fluids and gases have been given by Lorenz [9]. It is well-known that the sensitivity of the system to initial conditions is necessary for chaotic motion. In other words, it may happen that small differences in the initial conditions produce very great ones in final phenomena. Therefore prediction becomes impossible. Recently, many excellent books were given by Moon [10], Thompson and Stewart [11], Chen and Dong [12], and Kapitaniak [13]. Moreover, some outstanding works were also presented by El Naschie [14] and Kapitaniak [15].

Various interesting dynamic behaviors of a symmetric gyroscope mounted on a vibrating base have been found by Ge and Chen [4,5]. In the past study, the gyroscope was assumed to be rigid. A single equation of motion is used to analyze the dynamic behavior of the system; the system is viewed as a single-degree-of-freedom system. The gyroscope may not always be assumed to be a rigid body. In this paper, a two-degree-of-freedom system of a dissipative gyroscope mounted on a vibrating base is considered. Qualitative behaviors of the system are studied by center manifold theorem [16] and normal form theorem [17]. The co-dimension one and co-dimension two bifurcation analyses are presented. Further, numerical techniques are used to analyze the dynamic of this typical gyro. The time evolutions of the nonlinear dynamical system responses are described in phase portraits via the Poincaré maps. The occurrence and the nature of chaotic attractors are verified by evaluating the Liapunov exponents, and the Liapunov dimensions. Besides, the effect of the spin speed of the gyroscope is studied by numerical simulation in conjunction with Liapunov exponents, and it is shown that a chaotic motion will become regular as the spin speed of the gyroscope increases.

2. Formulation

The gyroscope contains a mechanical vibration absorber in the interior in the form of a spring-mass-dashpot. The absorber mass (m) is centered on the z axis and position parallel to z axis. The spring has constant k, and the dashpot has damping constant C. The geometry of the problem under consideration is depicted in Fig. 1. The motion of a symmetric gyroscope mounted on a vibrating base can be described by Euler's angles θ, ϕ and ψ. It is not difficult to show that the Lagrangian can be expressed as

$$L=\frac{1}{2}(I_1+mz^2)(\dot{\phi}^2+\dot{\theta}^2\sin^2\theta)+\frac{1}{2}I_3(\dot{\phi}\cos\theta+\dot{\psi})^2+\frac{1}{2}m\dot{z}^2-Mg(\ell+\bar{\ell}\sin\omega t)\cos\theta-mg(z+\bar{\ell}\sin\omega t)\cos\theta-\frac{k}{2}(z-\ell_0)^2, \tag{1}$$

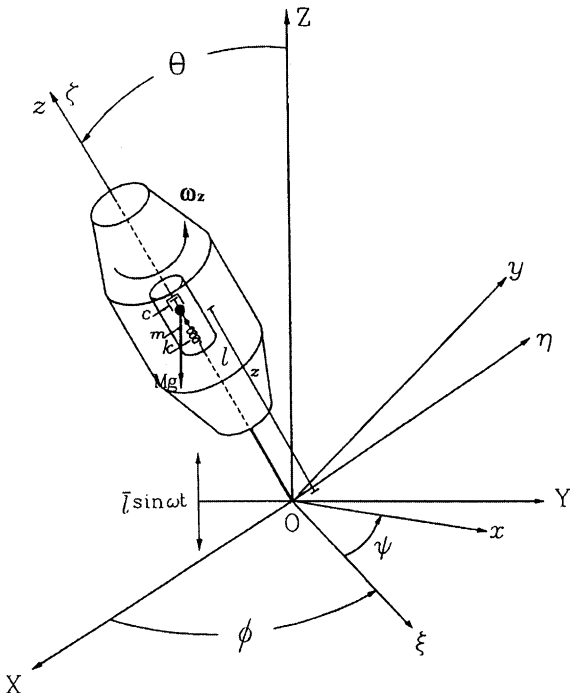

Fig. 1. A schematic diagram of a gyro.

where I_1, and I_3 are the polar and equatorial moments of inertia of the typical gyroscope, Mg is the gravity force, $\bar{\ell}$ is the amplitude of the external excitation disturbance, ω the frequency of the external excitation disturbance, m is the mass of the damper, and k the spring constant. It is clear that coordinates ϕ and ψ are cyclic, which provides us with two first integrals of the motion expressing the conjugate momenta. The momentum integrals are

$$P_\phi = \frac{\partial L}{\partial \dot{\phi}} = (I_1 + mz^2)\dot{\phi}\sin^2\theta + I_3(\dot{\phi}\cos\theta + \dot{\phi})\cos\theta = \beta_\phi, \tag{2}$$

$$P_\psi = \frac{\partial L}{\partial \dot{\psi}} = I_3(\dot{\phi}\cos\theta + \dot{\psi}) = I_3\omega_z = \beta_\psi, \tag{3}$$

where ω_z is the spin speed of the gyroscope.

Using the Routh's procedure via Eqs. (2) and (3), the Routhian of the system becomes

$$\begin{aligned} R &= L - \beta_\phi\dot{\phi} - \beta_\psi\dot{\psi} \\ &= \frac{1}{2}(I_1 + mz^2)\dot{\theta}^2 - \left[\frac{(\beta_\phi - \beta_\psi\cos\theta)^2}{2(I_1 + mz^2)\sin^2\theta} + \frac{\beta_\phi^2}{2I_3}\right] + \frac{1}{2}m\dot{z}^2 - Mg(\ell + \bar{\ell}\sin\omega t)\cos\theta - mg(z + \bar{\ell}\sin\omega t)\cos\theta \\ &\quad - \frac{1}{2}k(z - \ell_0)^2. \end{aligned} \tag{4}$$

For the trivial solution, from Eqs. (2) and (3), $\beta_\phi = \beta_\psi$ is automatically satisfied and is assumed to hold afterwards [18]. The dissipation function is given by

$$F = \frac{1}{2}C\dot{z}^2. \tag{5}$$

The equations of motion describing the system can be obtained from

$$\frac{\mathrm{d}}{\mathrm{d}t}\left(\frac{\partial R}{\partial \dot{q}_i}\right) - \frac{\partial R}{\partial q_i} + \frac{\partial F}{\partial \dot{q}_i} = 0, \quad \{q_i|\theta, z\}, \tag{6}$$

The system is viewed as a two-degree-of-freedom system. The equations governing the gyroscope are given by

$$\begin{cases} \ddot{\theta} + \frac{\beta_\phi^2}{(I_1+mz^2)^2}\frac{(1-\cos\theta)^2}{\sin^3\theta} - \left[\frac{Mg(\ell+\bar{\ell})\sin\omega t}{(I_1+mz^2)}\right]\sin\theta = 0, \\ \ddot{z} + \frac{C}{m}\dot{z} + k(z-\ell_0) - z(\dot{\theta}^2) + g\cos\theta - \frac{z\beta_\phi^2}{(I_1+mz^2)^2}\frac{(1-\cos\theta)^2}{\sin^2\theta} = 0. \end{cases} \tag{7}$$

The equilibrium point is found to be

$$\theta = 0, \quad \dot{\theta} = 0, \quad z = \left(\ell_0 - \frac{mg}{k}\right), \quad \dot{z} = 0. \tag{8}$$

For convenient analysis, the fixed point is shifted to the trivial one. The equation in first order form can be rewritten as

$$\begin{cases} \dot{x}_1 = x_2, \\ \dot{x}_2 = -\frac{\beta_\phi^2}{[I_1+m(x_3+p^2)]^2}\frac{(1-\cos x_1)}{\sin^3 x_1} + \frac{[(Mg\ell+mgp)+mgx_3+(M+m)g\bar{\ell}]\sin\omega t\sin x_1}{[I_1+m(x_3+p)^2]}, \\ \dot{x}_3 = x_4, \\ \dot{x}_4 = \left(\frac{\beta_\phi^2}{[I_1+m(x_3+p^2)]^2}\frac{(1-\cos x_1)^2}{\sin^2 x_1}\right)(x_3+p) + g(1-\cos x_1) - \frac{k}{m}x_3 + (x_3+p)x_2^2 - 2cx_4, \end{cases} \tag{9}$$

where

$$x_1 = \theta, \quad x_2 = \dot{\theta}, \quad x_3 = z - p, \quad x_4 = \dot{z}, \quad p = \ell_0 - \frac{mg}{k}, \quad 2c = \frac{C}{m}. \tag{10}$$

3. Stability analysis

3.1. The case of a pair of pure imaginary eigenvalues

In this subsection, the qualitative behaviors of the dissipative gyroscope system in the case, where the disturbance is absent, i.e., $\bar{\ell} = 0$ will be investigated. The study is concentrated on a co-dimension one bifurcation problem of the system. By Taylor's expansion, the equation of motion can be rewritten as

$$\begin{cases} \dot{x}_1 = x_2, \\ \dot{x}_2 = -\left[\frac{\beta_\phi^2}{4(I_1+mp^2)^2} - \frac{Mg\ell+mgp}{(I_1+mp^2)}\right]x_1 + a_1x_1x_3 + a_2x_1^3 + a_3x_1x_3^2 + \mathrm{O}(x_i^4), \\ \dot{x}_3 = x_4, \\ \dot{x}_4 = \frac{k}{m}x_3 - 2cx_4 + a_4x_1^2 + px_2^2 + px_3x_2^2 + a_5x_1^2x_3 + \mathrm{O}(x_i^4), \end{cases} \tag{11}$$

where

$$\begin{aligned} a_1 &= \frac{mgp}{(I_1+mp^2)} - \frac{(Mg\ell+mgp)(2mp)}{(I_1+mp^2)^2} + \frac{\beta_\phi^2}{(I_1+mp^2)^3}, \\ a_2 &= \frac{(Mg\ell+mgp)}{6(I_1+mp^2)} - \frac{\beta_\phi^2}{12(I_1+mp^2)^3}, \\ a_3 &= \frac{-2m^2gp}{(I_1+mp^2)^2} + \frac{(Mg\ell+mgp)(3m^2p^2-I_1m)}{(I_1+mp^2)^3} - \frac{(5m^2p^2-2mI_1)}{2(I_1+mp^2)^4}, \\ a_4 &= \frac{\beta_\phi^2 p}{4(I_1+mp^2)^2} - \frac{g}{2}, \quad a_5 = \frac{(I_1-3mp^2)}{4(I_1+mp^2)}. \end{aligned} \tag{12}$$

Eq. (11) is then rewritten in vector form as follows:

$$\dot{X} = AX + F(X) + \mathrm{O}(4), \tag{13}$$

where

$$X = [x_1, x_2, x_3, x_4]^{\mathrm{T}}, \quad F = [0, F_1, 0, F_2]^{\mathrm{T}}, \quad A = \begin{bmatrix} 0 & 1 & 0 & 0 \\ -\omega_1^2 & 0 & 0 & 0 \\ 0 & 0 & 0 & 1 \\ 0 & 0 & -\frac{k}{m} & -2c \end{bmatrix}, \tag{14}$$

and

$$\begin{aligned} \omega_1^2 &= \frac{\beta_\phi^2}{4(I_1+mp^2)^2} - \frac{Mg\ell+mgp}{4(I_1+mp^2)^2}, \\ F_1 &= a_1x_1x_3 + a_2x_1^3 + a_3x_1x_3^2, \quad F_2 = a_4x_1^2 + px_2^2 + px_3x_2^2 + a_5x_1^2x_3. \end{aligned} \tag{15}$$

From conventional linear stability analysis, one knows that in a certain parametric range the linearized system can be stable or unstable. However, the linearized system can only provide qualitative information on this nonlinear system in some cases, namely, when the eigenvalues of matrix A has no zero or purely imaginary values. A pair of purely imaginary eigenvalues is the major focus in the following analysis. The matrix A has complex eigenvalues $\lambda_1 = \omega_1\mathrm{i}$ and $\lambda_2 = -c + \omega_2\mathrm{i}$ (as well as $\bar{\lambda}_1 = -\omega_1\mathrm{i}$ and $\bar{\lambda}_2 = -c - \omega_2\mathrm{i}$), where

$$c^2 - \frac{k}{m} = -\omega_2^2. \tag{16}$$

To transform Eq. (13) into the form in which the center manifold theorem can be applied, the following linear transformation matrix:

$$B=\begin{bmatrix}0 & 1 & 0 & 0\\ \omega_1 & 0 & 0 & 0\\ 0 & 0 & 0 & 1\\ 0 & 0 & \omega_2 & -c\end{bmatrix} \tag{17}$$

is used. The matrix B is built from the eigenvectors of the matrix A. Let the coordinate transformation

$$X=Bq,\quad \text{where } q=[q_1,q_2,q_3,q_4]^{\mathrm{T}}. \tag{18}$$

Then Eq. (13) is transformed as

$$\dot{q}=B^{-1}ABq+B^{-1}F(q)+\mathrm{O}(4). \tag{19}$$

The detailed expression is

$$\begin{bmatrix}\dot{q}_1\\ \dot{q}_2\\ \dot{q}_3\\ \dot{q}_4\end{bmatrix}=\begin{bmatrix}0 & -\omega_1 & 0 & 0\\ \omega_1 & 0 & 0 & 0\\ 0 & 0 & -c & -\omega_2\\ 0 & 0 & \omega_2 & -c\end{bmatrix}\begin{bmatrix}q_1\\ q_2\\ q_3\\ q_4\end{bmatrix}+\begin{bmatrix}F_1(q_i)\\ 0\\ F_2(q_i)\\ 0\end{bmatrix}+\mathrm{O}(4), \tag{20}$$

where

$$\begin{aligned}F_1&=\frac{1}{\omega_1}(a_1q_2q_4+a_2q_2^3+a_3q_2q_4^2),\\ F_2&=\frac{1}{\omega_2}(a_4q_2^2+p\omega_1^2q_1^2+p\omega_1^2q_1^2q_4+a_5q_2^2q_4).\end{aligned} \tag{21}$$

Search for a two-dimensional center manifold:

$$\begin{aligned}q_3&=h_1(q_1,q_2)=S_1q_1^2+S_2q_1q_2+S_3q_2^2+\mathrm{O}(3),\\ q_4&=h_2(q_1,q_2)=T_1q_1^2+T_2q_1q_2+T_3q_2^2+\mathrm{O}(3).\end{aligned} \tag{22}$$

According to the center manifold theorem, the following:

$$\begin{cases}\frac{\partial h_1}{\partial q_1}[-\omega_1q_2+F_1(q_1,q_2,h_1,h_2)]+\frac{\partial h_1}{\partial q_2}(\omega_1q_1)-(-ch_1-\omega_2h_2)-F_2(q_1,q_2,h_1,h_2)=0,\\ \frac{\partial h_2}{\partial q_1}(-\omega_1q_2)+\frac{\partial h_2}{\partial q_2}(\omega_1q_1)-(-ch_2-\omega_2h_1)=0\end{cases} \tag{23}$$

must be satisfied. Equating powers of q_1^2, q_1q_2, q_2^2, one obtains that

$$\begin{bmatrix}c & \omega_1 & 0 & \omega_2 & 0 & 0\\ 0 & -\omega_1 & c & 0 & 0 & \omega_2\\ -2\omega_1 & c & 2\omega_1 & 0 & \omega_2 & 0\\ -\omega_2 & 0 & 0 & c & \omega_1 & 0\\ 0 & -\omega_2 & 0 & -2\omega_1 & c & 2\omega_1\\ 0 & 0 & -\omega_2 & 0 & -\omega_1 & c\end{bmatrix}\begin{bmatrix}S_1\\ S_2\\ S_3\\ T_1\\ T_2\\ T_3\end{bmatrix}=\begin{bmatrix}p\omega_1^2/\omega_2\\ a_4/\omega_2\\ 0\\ 0\\ 0\\ 0\end{bmatrix}. \tag{24}$$

By Cramer's rule, the solution of the non-homogeneous linear set of equations can be obtained. We define

$$S_1=S_1^*,\quad S_2=S_2^*,\quad S_3=S_3^*,\quad T_1=T_1^*,\quad T_2=T_2^*,\quad T_3=T_3^*, \tag{25}$$

thus one has

$$\begin{aligned}q_3&=h_1(q_1,q_2)=S_1^*q_1^2+S_2^*q_1q_2+S_3^*q_2^2+\mathrm{O}(3),\\ q_4&=h_2(q_1,q_2)=T_1^*q_1^2+T_2^*q_1q_2+T_3^*q_2^2+\mathrm{O}(3).\end{aligned} \tag{26}$$

Substituting Eq. (26) into (20), the reduced system, which determines stability, is therefore given by

$$\begin{bmatrix}\dot{q}_1\\ \dot{q}_2\end{bmatrix}=\begin{bmatrix}0 & -\omega_1\\ \omega_1 & 0\end{bmatrix}\begin{bmatrix}q_1\\ q_2\end{bmatrix}+\begin{bmatrix}\omega_1^{-1}[a_1T_1^*q_1^2q_2+a_1T_2^*q_2^2q_1+(a_1T_3^*+a_2)q_2^3]\\ 0\end{bmatrix}+\mathrm{O}(5). \tag{27}$$

The center manifold theorem has been applied to this system. Up to now, the stability of the system is undetermined, thus the normal form theorem will be adopted to study this problem afterwards. The normal form theorem implies that many nonlinear terms in Eq. (27) can be removed by a nonlinear transformation and this transformation does not affect the qualitative behavior of the system. The normal form theorem gives a coordinate transformation which transforms the system (27) into the following system:

$$\begin{bmatrix}\dot{y}_1\\ \dot{y}_2\end{bmatrix}=\begin{bmatrix}0 & -\omega_1\\ \omega_1 & 0\end{bmatrix}\begin{bmatrix}y_1\\ y_2\end{bmatrix}+\begin{bmatrix}(\Lambda_1 y_1+\Lambda_2 y_2)(y_1^2+y_2^2)\\ (\Lambda_1 y_2-\Lambda_2 y_1)(y_1^2+y_2^2)\end{bmatrix}+\mathrm{O}(5), \tag{28}$$

where

$$\Lambda_1=\frac{a_1T_2^*}{8\omega_1},\quad \Lambda_2=\frac{1}{8}\left[\frac{a_1T_1^*}{\omega_1}+\frac{3(a_1T_3^*+a_2)}{\omega_1}\right]. \tag{29}$$

In the absence of the terms of order O(5), the local family (29) is more tractable in plane polar coordinates (r,Θ). It is easily shown that

$$\dot{r}=r(\mu+\Lambda_1)r^2,\quad \dot{\Theta}=\omega_1-\Lambda_2 r^2. \tag{30}$$

Let us assume that $\Lambda_1<0$. The phase portrait of the system (30) for $\mu<0$ consists of a hyperbolic, stable focus at the origin. When $\mu=0$, $\dot{r}=\Lambda_1 r^3$ and the origin is still asymptotically stable, though it is no longer hyperbolic. For $\mu>0$, $\dot{r}=0$ for $r=\sqrt{\mu/|\Lambda_1|}$ as well as for $r=0$. It follows that for $\mu>0$ there is a stable limit cycle, of radius proportional to $\sqrt{\mu}$, surrounding a hyperbolic, unstable focus at the origin. This is called a supercritical Hopf bifurcation; the authors refer the reader to Thompson and Stewart [11]. If $\Lambda_1>0$, then the limit cycle occurs for $\mu<0$: it is unstable and surrounds a stable fixed point. As μ increases, the radius of the limit cycle decreases to zero at $\mu=0$, where the fixed point at the origin becomes a weakly unstable focus. For $\mu>0$, $(y_1,y_2)^T=0$ is unstable and hyperbolic. This is known as a subcritical Hopf bifurcation.

3.2. The case of a double zero eigenvalues

When $\omega_1=0$ the matrix A has a double zero eigenvalues, and a pair of complex eigenvalues with negative real parts. Similarly, the center manifold theorem is used to reduce the original-dimensional equation to a two-dimensional one to simplify the analysis. The center manifolds are found as follows:

$$\begin{aligned}x_3&=h_1(x_1,x_2)=\frac{a_4}{c^2+\omega_2^2}x_1^2-\frac{4a_4c}{(c^2+\omega_2^2)^2}x_1x_2+\frac{1}{c^2+\omega_2^2}\left(p+\frac{8a_4c^2}{(c^2+\omega_2^2)^2}-\frac{2a_4}{c^2+\omega_2^2}\right)x_2^2,\\ x_4&=h_2(x_1,x_2)=\frac{2a_4}{c^2+\omega_2^2}x_1x_2-\frac{4a_4c}{(c^2+\omega_2^2)^2}x_2^2.\end{aligned} \tag{31}$$

Then, the reduced system is obtained as

$$\begin{aligned}\dot{x}_1&=x_2,\\ \dot{x}_2&=\frac{a_1a_4}{c^2+\omega_2^2}x_1^3-\frac{4a_1a_4c}{(c^2+\omega_2^2)^2}x_1^2x_2+\frac{a_1}{c^2+\omega_2^2}\left(p+\frac{8a_4c^2}{(c^2+\omega_2^2)^2}-\frac{2a_4}{c^2+\omega_2^2}\right)x_1x_2^2,\end{aligned} \tag{32}$$

Next, the above reduced system will be transformed to the simplest form, known as the normal form. This is given by

$$\begin{aligned}\dot{y}_1&=y_2,\\ \dot{y}_2&=\alpha_1y_1^3+\alpha_2y_1^2y_2,\end{aligned} \tag{33}$$

where

$$\alpha 1=\frac{a_1a_4}{c^2+\omega_2^2},\quad \alpha_2=\frac{-4a_1a_4c}{(c^2+\omega_2^2)^2}. \tag{34}$$

The unfolding of the normal form is given as

$$\begin{aligned}\dot{y}_1&=y_2,\\ \dot{y}_2&=\mu_1y_1+\mu_2y_2+\alpha_1y_1^3+\alpha_2y_1^2y_2.\end{aligned} \tag{35}$$

It is easy to find that Eq. (35) has fixed points at

$$A : (y_1, y_2) = (0, 0), \quad B : (y_1, y_2) = \left(\pm\sqrt{\frac{-\mu_1}{\alpha_1}}, 0\right). \tag{36}$$

It is not difficult to determine the stabilities of these fixed points. For point A, when $\mu_2 > 0$ and $\mu_2^2 + 4\mu_1 > 0$, the equilibrium is a saddle. If $\mu_2 > 0$ and $\mu_2^2 + 4\mu_1 < 0$, then the point A is a source. If $u_2 < 0$ and $\mu_2^2 + 4\mu_1 > 0$, it is known that this point is a saddle point. If $\mu_2 < 0$ and $\mu_2^2 + 4\mu_1 < 0$, then this point A is a sink. Further, the supercritical pitchfork bifurcations occur on the line $\mu_1 = 0$, the Hopf bifurcations occur when $\mu_1 < 0$ and $\mu_2 = 0$. For point B, when $\mu_2 - \mu_1 > 0$ and $\mu_1 > 0$ the equilibrium is a source. When $\mu_2 - \mu_1 > 0$ and $\mu_1 < 0$ the equilibrium is a saddle point. If $\mu_2 - \mu_1 < 0$ and $\mu_1 > 0$, then the point B is a sink. If $\mu_2 - \mu_1 < 0$ and $\mu_1 < 0$, then the point B is a saddle point. Besides, the supercritical pitchfork bifurcation occurs on the line $\mu_1 = 0$. Again it is found that a secondary bifurcation cannot occur.

Further, the so-called saddle connection bifurcation must be examined by the rescaling and the Melnikov method. The rescaling transformation is introduced as follows:

$$y_1 = \varepsilon\mu, \quad y_2 = \varepsilon^2 v, \quad \mu_1 = \varepsilon^2 v_1, \quad \mu_2 = \varepsilon^2 v_2. \tag{37}$$

This brings the system to the form of

$$\begin{aligned} \dot{\mu} &= v, \\ \dot{v} &= v_1 M + \alpha_1 M^3 + \varepsilon(v_2 v + \alpha_2 \mu^2 v). \end{aligned} \tag{38}$$

For $\varepsilon = 0$, the Hamiltonian function is

$$H(\mu, v) = \frac{v^2}{2} - \frac{v_1 v^2}{2} - \frac{\alpha_1 \mu^4}{4}. \tag{39}$$

Simply, let $v_1 = -\alpha_2$, the system (39) has a pair of saddle points $(\mu, v) = (\pm 1, 0)$, and the heteroclinic orbits are

$$\mu_0 = \pm\sqrt{2}\operatorname{sech}\sqrt{\alpha_1 t}, \quad v_0 = \mp\sqrt{2\alpha_1}(\operatorname{sech}\sqrt{\alpha_1 t})\tanh\sqrt{\alpha_1 t}. \tag{40}$$

From the Melnikov function, when the saddle connection is preserved, the following condition:

$$M(v_2) = \int_{-\infty}^{\infty} v_0(v_2 v_0 + \alpha_2 \mu_0^2 v_0)\,\mathrm{d}t = 0. \tag{41}$$

must be satisfied. From the above condition, one obtains

$$v_2 = \frac{-\alpha_2}{5\sqrt{\alpha_1}}. \tag{42}$$

Returning the unsealed parameters, the final criterion for the saddle connection is

$$\frac{\mu_1}{\mu_2} = \frac{5\sqrt[3]{\alpha_1^2}}{\alpha_2}. \tag{43}$$

This completes the local analysis of the system in the neighborhood of the bifurcation.

4. Numerical simulations and discussion

In order to simplify the analysis, most of the parameters are kept constant. The parameter values are: $I_1 = 1.0$, $k = 100$, $\ell = 0.1$, $M = 0.5$, $m = 0.1$, $p = 0.1$, $\beta_\phi^2 = 100$, $\omega = 2.0$, $2c = 0.5$. The only varied parameter is $\bar{\ell}$. Solutions of Eq. (9) are obtained using a Runge–Kutta integration algorithm, with the time step size of 0.01, and different initial conditions. From the numerical integration of Eq. (9), phase plane plots and corresponding Poincaré maps, can easily be constructed and Liapunov exponents calculated. For some different parameter values, the system under consideration can be driven into chaos. In this study, the powerful Liapunov exponent tests are shown in Fig. 2 to confirm the chaotic motion. As $\bar{\ell} < 4.68$, the system exhibits regular motion; when $\bar{\ell} > 4.68$, it routes to chaotic motion.

The Poincaré map in Fig. 3 is a closed curve, which indicates that the motion is quasi-periodic. Fig. 4 shows the Poincaré map, which corresponds to a typical chaotic attractor. The Poincaré maps provide an interesting strange attractor on which the motion is possibly unpredictable. It is found that a quasi-periodic behavior can be changed into a chaotic motion as the forcing amplitude increases. Fig. 5 also shows the time history of a quasi-periodic oscillation for $\bar{\ell} = 2.0$. Fig. 6 also displays the time history of a chaotic oscillation of the gyroscope for $\bar{\ell} = 5.0$.

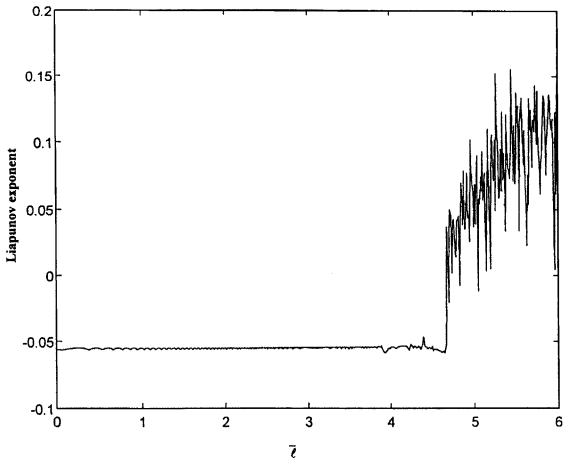

Fig. 2. The largest Liapunov exponent as a function of $\bar{\ell}$ for a dissipative gyro.

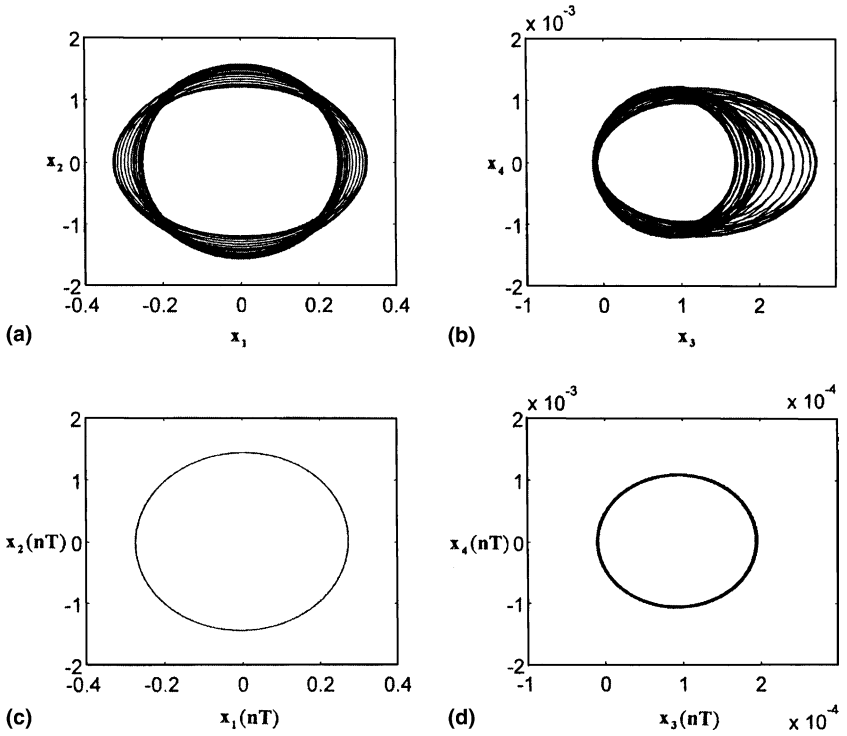

Fig. 3. (a), (b) The phase trajectory for $\bar{\ell} = 2.0$; (c), (d) The Poincaré maps for $\bar{\ell} = 2.0$.

The spectral analysis of the Liapunov exponents has proven to be the most useful dynamical diagnostic for chaotic system. The spectrum of the Liapunov exponents enables one to classify the system attractor, its dimension and the sensitivity of the system to initial conditions. The numerical calculations have been undertaken by using the method described in Wolf et al. [19]. Time plays the role of one of the dimensions and in this direction the exponent is always zero. The Liapunov exponents spectrum for any chaotic oscillation in four-dimensional phase space can be (+, 0, −, −), (+, +, 0, −) or (+, 0, 0, −). The occurrence of two or more positive Liapunov exponents is called hyperchaos. In this study, the Liapunov exponents spectrum for chaotic oscillation is the type (+, 0, −, −). Hyperchaos is not found in this research. The largest Liapunov exponents obtained for the system as a function of $\bar{\ell}$ are plotted in Fig. 2. The sum of the

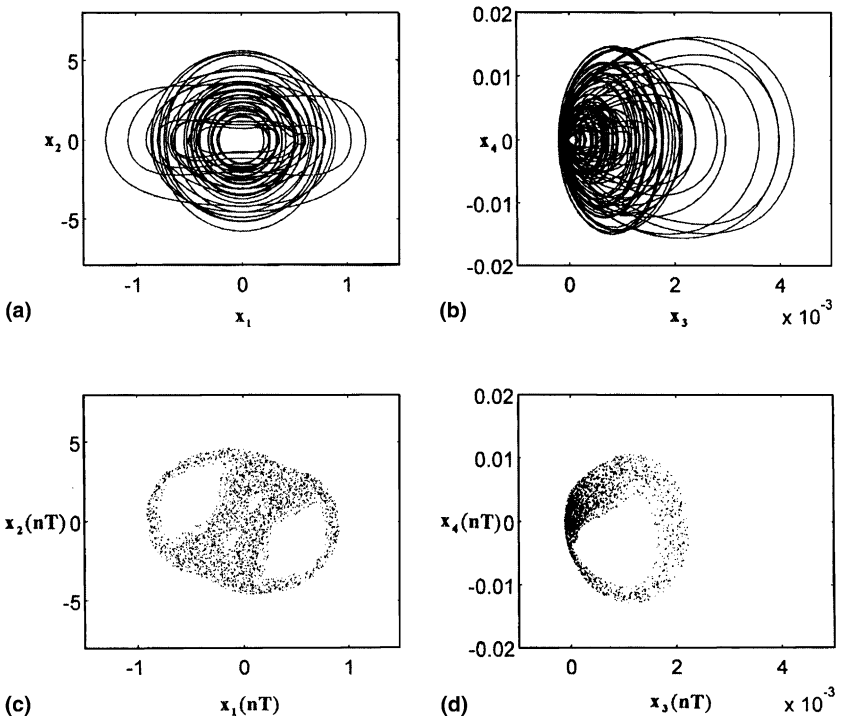

Fig. 4. (a), (b) The phase trajectory for $\bar{\ell} = 5.0$; (c), (d) The Poincaré maps for $\bar{\ell} = 5.0$.

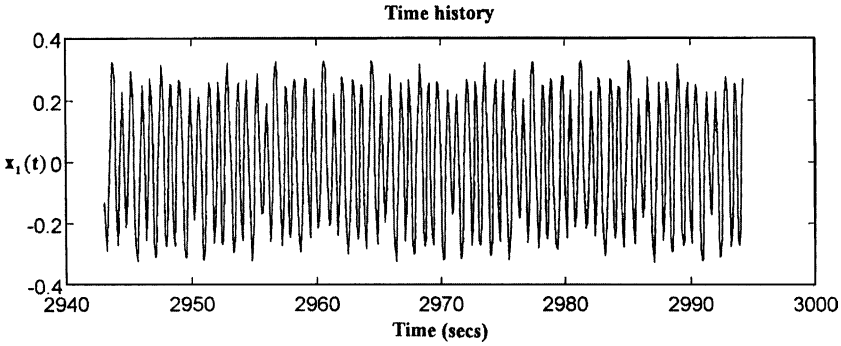

Fig. 5. The time history for $\bar{\ell} = 2.0$.

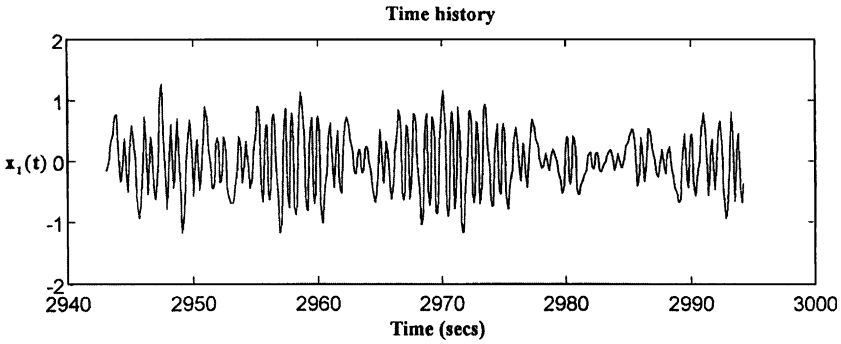

Fig. 6. The time history for $\bar{\ell} = 5.0$.

four Liapunov exponents is negative and it approaches to -0.5. For example, at the following parameters: $I_1 = 1.0$, $k = 100$, $\ell = 0.1$, $\bar{\ell} = 5.0$, $M = 0.5$, $m = 0.1$, $p = 0.1$, $\beta_\phi^2 = 100$, $\omega = 2.0$, $2c = 0.5$, the calculated Liapunov exponents are $\lambda_1 = 0.072$, $\lambda_2 = 0$, $\lambda_3 = -0.277$, $\lambda_4 = -0.295$. The sum of the exponents is $\sum \lambda = -0.5$. The dimension of an attractor reflects one of the essential aspects of dissipative dynamics; that is, the contraction of the phase volume. A chaotic attractor is federated by contraction accompanied by stretching and folding of the state trajectories, it has a non-integer

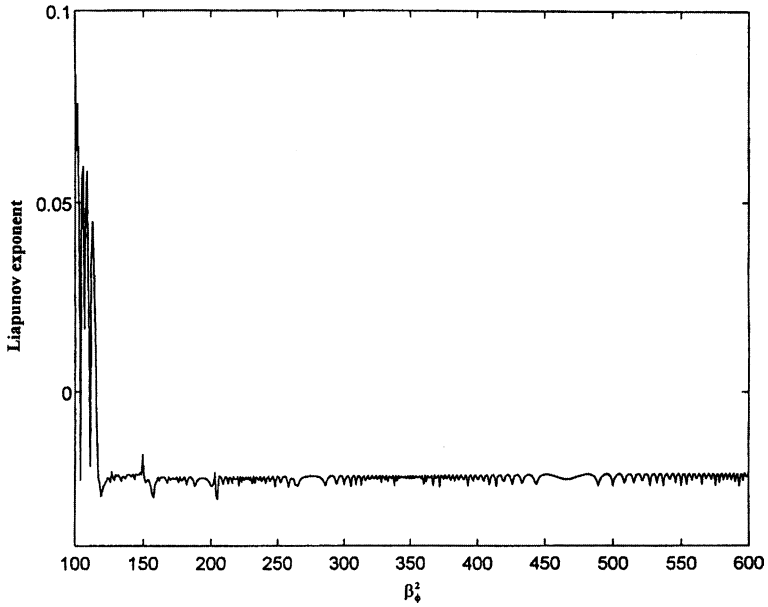

Fig. 7. The largest Liapunov exponent as a function of $\beta_\phi^2 (\beta_\phi = I_3\omega_z/I_1)$ for $\bar{\ell} = 5.0$.

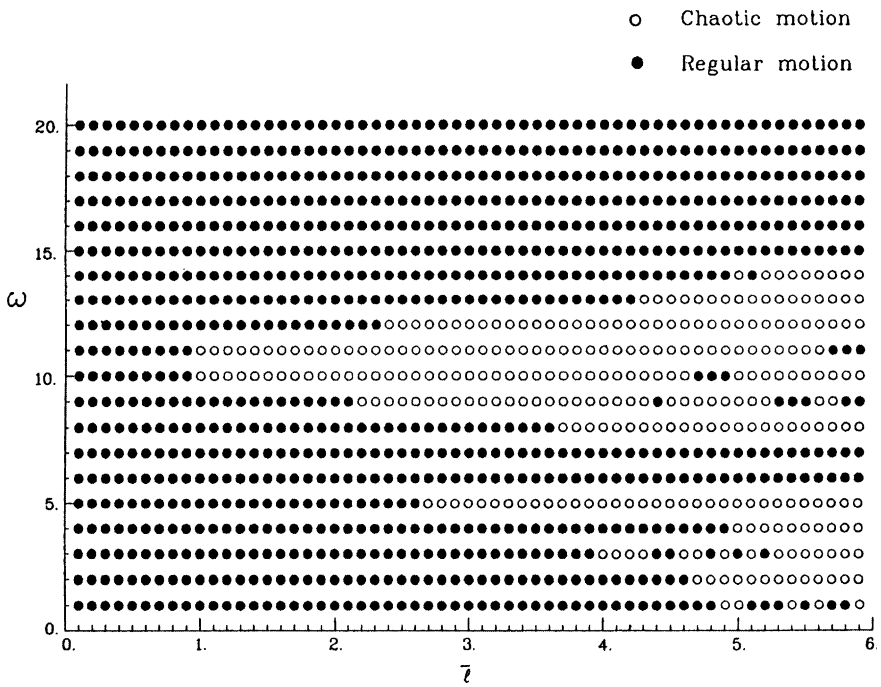

Fig. 8. Parametric diagram of $\bar{\ell}$ versus forcing frequency ω.

dimension. The Liapunov dimension dL can be obtained, according to the definition given by Kaplan and Yorke [20]. The calculated fractal dimension of the above chaotic attractor is 3.126.

The governing equations contain various different parameters. Obviously, it is not feasible to study the effects of the all these parameters. A few interesting cases are presented below. The associated parameter values are given in the figure captions. According to past experience in studying the gyroscope, the effect of the spin speed of the gyroscope on the system behavior plays an important role. Here the effect of the spin speed of the gyroscope on the dynamic behaviors of the system is studied by numerical simulation in conjunction with the Liapunov spectrum analysis. Fig. 7 shows that when the spin speed of the gyroscope increased, the chaotic motion disappears, and regularity returns. Further a parameter diagram for ω and $\bar{\ell}$ showing the regular and chaotic motions is plotted in Fig. 8.

5. Conclusions

The nonlinear motion of a dissipative symmetric gyroscope has been investigated qualitatively and numerically. It has been shown by computer simulation that, for this two-degree-of-freedom system, quasi-periodic and chaotic behavior exists for certain values of the amplitude and the frequency of the base excitation. Quasi-periodic routes to chaos in the system have also been observed. The qualitative behaviors of the system have been studied by the center manifold theorem and the normal form theorem in Section 3. The co-dimension one bifurcation analysis for the Hopf bifurcation has been carried out. The pitchfork, Hopf, and the saddle connection bifurcation for co-dimension two bifurcation have been found. The quasi-periodic and chaotic behaviors have been described in the phase plane. In addition to the Poincaré maps and the Liapunov exponents have been computed numerically and the related fractal dimensions have been used to show the presence of chaotic behavior in the system. Besides, the effect of the spin speed of the gyroscope on its dynamic behavior has also been considered. It has been found that the higher spin speed of the gyroscope can quench the chaotic motion in this study. It can be effectively used in controlling chaos. Our findings can be quite beneficial to further understanding and utilization of the complex gyroscope.

Acknowledgment

This research is supported by the National Science Council, Republic of China, under Grant Number NSC88-2212-E-009-001.

References

[1] Leipnik RB, Newton TA. Double strange attractors in rigid body motion. Phys Lett A 1981;86:63–7.
[2] Ge ZM, Chen HH. Bifurcation and chaotic motions in a rate gyro with sinusoidal velocity about spin axis. J Sound Vibr 1997;200:121–37.
[3] Ge ZM, Chen HH. Bifurcations and chaos in a rate gyro with harmonic excitation. J Sound Vibr 1996;194:107–17.
[4] Ge ZM, Chen HK, Chen HH. The regular and chaotic motions of a symmetric heavy gyroscope with harmonic excitation. J Sound Vibr 1996;198:131–47.
[5] Ge ZM, Chen HK. Stability and chaotic motions of a symmetric heavy gyroscope. Jpn J Appl Phys 1996;35:1954–65.
[6] Tong X, Mrad N. Chaotic motion of a symmetric gyro subjected to a harmonic base excitation. Trans ASME J Appl Mech 2001;68:681–4.
[7] Chen HK, Lee CI. Anti-control of chaos in rigid body motion. Chaos, Solitons & Fractals 2004;21:957–65.
[8] Poinearé H. Les Methodes Nouvelles de La Mecanique. Paris: Gauthier-Villiars; 1899.
[9] Lorenz EN. Deterministic non-periodic flows. J Atmosphere Sci 1963;20:130–41.
[10] Moon FC. Chaotic and Fractal Dynamics. New York: Wiley; 1992.
[11] Thompson JMT, Stewart HB. Nonlinear Dynamics and Chaos. New York: John Wiley & Sons; 1987.
[12] Chen G, Dong X. From Chaos to Order: Methodologies, Perspectives and Applications. Singapore: World Scientific; 1998.
[13] Kapitaniak T. Chaos for Engineers: Theory, Application and Control. Berlin: Springer; 1998.
[14] El Naschie MS. Introduction to chaos, information and diffusion in quantum physics. Chaos, Solitons & Fractals 1996;7:7–10.
[15] Kapitaniak T. Controlling chaotic oscillations without feedback. Chaos, Solitons & Fractals 1992;2:519–30.
[16] Carr J. Applications of Center Manifold Theory. New York: Springer-Verlag; 1981.
[17] Wiggins S. Global Bifurcations and Chaos. New York: Springer-Verlag; 1988.
[18] Gantmacher FR. Lectures on Analytic Mechanics. Moscow: Gosudarstvennoe Izdat'elstvo FizikoMat'emat'iskoi Literaturi; 1960.

[19] Wolf A, Swift JB, Swinney HL, Vastano JA. Determining Liapunov exponents from a time series. Physica D 1985;16: 285–317.
[20] Kaplan H, Yorke JA. Lecture Note in Mathematics. Berlin: Springer-Verlag; 1979.